Dynamic Load Behavior During Power Restoration: An Aggregated Modeling Approach

Johanna Timmermann, Carolin Vogel, Xinyu Liu, Reinaldo Tonkoski and Rolf Witzmann
Chair of Electric Power Transmission and Distribution
Technical University of Munich
Munich, Germany
{johanna.timmermann; carolin.vogel}@tum.de

***Abstract*—The proposed load modeling approach integrates three complementary components: a dynamic load model, a Cold Load Pickup (CLPU) model and a simplified RMS-domain transformer inrush model. Dynamic load model parameters are derived for three distribution grid types: semi-urban, industrial and rural. By applying structure-preserving seasonal and diurnal scaling factors, the approach ensures consistency with a given reference dataset while retaining specific dynamic load characteristics. The resulting output is a multi-dimensional parameter set resolved by grid type, season and time of day. The CLPU model captures load recovery dynamics following supply restoration, while the transformer inrush model employs an exponential decay function to approximate the transient current peak and its decay toward steady-state conditions. Together, these components enable consistent RMS-domain studies that account for both load restoration and transformer energization effects.**

***Index Terms*—Cold load pick up, dynamic load modeling, power restoration, system dynamics, transformer inrush current**

I. Introduction

Accurate representation of load behavior under varying grid conditions remains a fundamental aspect of modern power system modeling and simulation. While load behavior is inherently diverse and time-dependent, simulation tools require parameter sets that remain both representative and computationally tractable. The identification of reliable model parameters is crucial for their application. Deriving parameter sets that adequately capture temporal, seasonal and regional diversity continues to pose a significant challenge, where both measurement-based and component-based identification techniques are commonly used. Measurement-based approaches, such as offline and recursive least squares or Kalman filtering, estimate static and dynamic load model parameters using high-resolution measurement data [1]. In contrast, component-based approaches rely on manufacturer data sheets, laboratory experiments or targeted field trials to construct composite load representations from known equipment characteristics [2]. Both IEEE and CIGRÉ have promoted hybrid frameworks that combine measurement-based and component-based approaches. Supported by open-source tool chains and standardized data formats, such hybrid methods streamline model validation, foster collaborative research and enhance the reproducibility of load modeling practices across the industry [1]. However, the required high-quality measurement data for power restoration scenarios are largely unavailable.

A general load modeling expression, capturing static and dynamic voltage- and frequency-dependent effects during restoration, has been introduced by [3]. Using empirical exponential terms, it does not employ explicit ZIP formulations or account for fast transients such as transformer inrush currents. To address these gaps, this paper proposes an aggregated load modeling framework for dynamic power restoration studies. It introduces a hybrid ZIP–dynamic–inrush model and demonstrates the model parameterization process based on literature data. The paper is organized as follows: Section II presents the proposed aggregated load modeling approach, describing each model component separately. Section III details the identification of model parameter sets for each component. Section IV concludes the paper with key findings and limitations.

II. Proposed Aggregated Load Modeling Approach for Dynamic Power Restoration Studies

Fig. 1 illustrates the proposed modeling framework for RMS-domain simulations. It combines a dynamic load model, capturing voltage and frequency dependencies, and CSV-based time series of active and reactive power that reproduce the effects of Cold Load Pickup (CLPU) and transformer inrush. Where CLPU refers to a temporary surge in demand that occurs when previously de-energized and diversified loads are being simultaneously restored after an outage [4]. This setup provides a comprehensive representation of load and transformer behavior during post-outage recovery while accounting for the load's inherent voltage- and frequency-dependent behavior and the corresponding system response. With this, the proposed model supports grid restoration studies and is suitable for representing lumped low-voltage loads, where detailed composition data are often unavailable and parameter estimation is challenging. One notable benefit of this approach is the reduced number of parameters compared to alternative load models, such as composite load models [1].

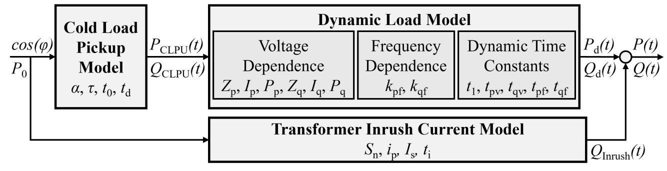

Fig. 1. Schematic of the aggregated load model for power restoration studies.

979-8-3315-8138-1

The subsequent sections outline each core component of the framework separately, and provide representative parameter ranges to facilitate each component's practical application.

A. *Dynamic Load Model*

1) Voltage Dependence - ZIP Model: The polynomial ZIP model decomposes the load's demand into three components: constant-impedance (Z), constant-current (I) and constant-power (P). The load's active and reactive power demand are expressed as functions of the bus voltage magnitude v [5], [6]:

$$P(v) = P_0 \left(Z_\mathrm{p} \left(\frac{v}{v_0} \right)^2 + I_\mathrm{p} \left(\frac{v}{v_0} \right)^1 + P_\mathrm{p} \left(\frac{v}{v_0} \right)^0 \right) \quad (1)$$

$$\text{with } Z_\mathrm{p} + I_\mathrm{p} + P_\mathrm{p} = 1$$

$$Q(v) = Q_0 \left(Z_\mathrm{q} \left(\frac{v}{v_0} \right)^2 + I_\mathrm{q} \left(\frac{v}{v_0} \right)^1 + P_\mathrm{q} \left(\frac{v}{v_0} \right)^0 \right) \quad (2)$$

$$\text{with } Z_\mathrm{q} + I_\mathrm{q} + P_\mathrm{q} = 1$$

Here, P_0 and Q_0 are the load's active and reactive power demand at nominal voltage v_0, and $Z_{\mathrm{p/q}}$, $I_{\mathrm{p/q}}$ and $P_{\mathrm{p/q}}$ depict the proportion of the respective ZIP model components. In the proposed aggregated modeling approach, the ZIP model represents the load's static voltage dependent characteristics. However, it does not capture the load's frequency-dependent behavior or any dynamics, which are addressed separately.

2) Frequency Dependence: The steady-state variations of the load's active and reactive power demand in response to deviations from the nominal frequency f_0 are calculated as:

$$P(f) = P_0 \left(1 + k_\mathrm{pf} \frac{f - f_0}{f_0} \right) \quad (3)$$

$$Q(f) = Q_0 \left(1 + k_\mathrm{qf} \frac{f - f_0}{f_0} \right) \quad (4)$$

where the factors k_{pf} and k_{qf} represent the sensitivities of the active and reactive power demand to a change in frequency [7].

3) Dynamics - Time Constants: The dynamic load model in DIgSILENT PowerFactory is shown in Fig. 2, where the load's active and reactive power demand, P_d and Q_d, are determined based on deviations in frequency Δf and voltage Δv [6].

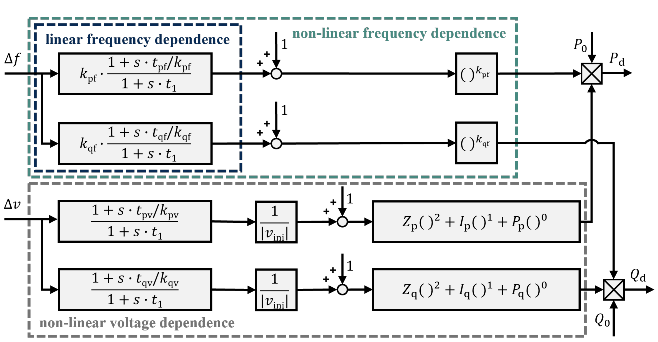

Fig. 2. Dynamic load model in DIgSILENT PowerFactory, according to [6].

B. *Cold Load Pickup Model*

Studies show that CLPU appears as a sharp post-restoration load spike, exceeding normal steady-state levels, followed by gradual decay [8], [9]. In future low-carbon scenarios, peak CLPU loads may even double normal levels and last tens of minutes, depending on load composition and environmental factors [10]. This can reduce generator efficiency, stress transformers and trigger secondary outages [11]. Failing to account for CLPU uncertainty can compromise system stability and hinder restoration, especially during large-scale outages.

The overview in [12] consolidates existing CLPU modeling approaches and parameterization methodologies, offering a comparative perspective. Due to their simplicity and ease of parameterization from field data, Exponential Decay (ED) and Delayed Exponential Decay (DED) models, as shown in (5) and (6), are widely used to capture CLPU behavior [4], [13]. Developed for aggregated LV loads rather than individual elements, these models inherently capture the combined response of load components both affected and unaffected by CLPU. Both effectively approximate the temporary surge in the aggregated load demand after restoration, with the ED model assuming an immediate active power overshoot that exponentially decays over time, as formulated in [4]:

$$P_\mathrm{CLPU}(t) = P_0 \cdot \left(1 + \alpha\, e^{-\frac{t - t_0}{\tau}} \right), \quad t > t_0 \quad (5)$$

where P_0 is the steady-state load, α the overshoot magnitude, τ the decay time constant and t_0 the load re-connection time. While the ED model captures the general load recovery trend, it fails to represent cases where the load's demand remains elevated before decaying (e.g., thermostatically controlled loads). The DED model adresses this by introducing a delay t_d, during which the load remains at its peak, as formulated in [4]:

$$P_\mathrm{CLPU}(t) = \begin{cases} P_0 \cdot (1 + \alpha), & 0 < t \leq t_\mathrm{d} \\ P_0 \cdot \left(1 + \alpha\, e^{-\frac{t - t_0 - t_\mathrm{d}}{\tau}} \right), & t > t_\mathrm{d} \end{cases} \quad (6)$$

Further, reactive power during CLPU can be approximated by assuming a constant power factor offering a simple yet effective means to estimate time-varying reactive power when detailed data are unavailable. Given the active power from (6) and the phase angle φ, the reactive power is calculated as:

$$Q_\mathrm{CLPU}(t) = P_\mathrm{CLPU}(t) \cdot tan(\varphi) \quad (7)$$

Beyond ED and DED models, advanced CLPU modeling approaches have been proposed to capture load restoration behavior more accurately. For instance, approaches employing decision-dependent uncertainty frameworks [14], multi-state load models [15] or data-driven frameworks to assess cold load pickup demand [11]. However, these methods demand detailed appliance data, real-time monitoring or intensive computation. Whereas, with only a small set of parameters, the DED model effectively captures key CLPU characteristics, peak persistence and exponential decay, making it suitable for aggregated load modeling and restoration studies under limited data conditions.

979-8-3315-8138-1

C. Transformer Inrush Current Model

Transformer energization is a transient phenomenon of significant importance in power restoration studies. The sudden inrush of magnetizing current following switch-on can reach several times the rated current, potentially causing voltage sags, mechanical stress and misoperation of protection devices. Factors such as the circuit closing angle and residual magnetic flux are dominant in determining the inrush current characteristics [17]–[19]. Many existing transformer inrush models include nonlinear and harmonic components, an exponential decay term is often embedded in the transient current expression [18]–[21]. In this work, inspired by [19], where per-cycle peak currents are evaluated, a simplified model for RMS studies is developed based on measured transformer inrush data. The transient inrush current is modeled using an exponential decay function to approximate the current magnitude envelope over time, capturing the rapid initial current peak and the subsequent decay. This formulation represents only the transient inrush behavior and does not include the steady-state load current. It enables the inclusion of inrush dynamics in RMS simulations without detailed electromagnetic transient modeling and provides an efficient means for assessing the impact of transformer energization on protection coordination and reactive power performance. The inrush is modeled as:

$$i_{\mathrm{Inrush}}(t) = I_{\mathrm{S}} \cdot (i_{\mathrm{p}} - 1)\, e^{-t/t_i} \tag{8}$$

$$\text{where } i_{\mathrm{p}} = I_{\mathrm{Peak}} / I_{\mathrm{S}} \tag{9}$$

is the dimensionless ratio of the cycle-by-cycle peak inrush current I_{Peak} to the steady-state current I_{S}, and t_{i} is the decay time constant. Using the ratio i_{p} allows scaling the inrush peak with respect to the load-dependent steady-state current. For transformer magnetizing inrush, the active power is considered negligible ($P_{\mathrm{Inrush}} = 0$) as the magnetizing current is predominantly reactive and does not significantly contribute to real power transfer [22]. Consequently, the reactive power Q_{Inrush} is computed directly from the inrush current magnitude as:

$$Q_{\mathrm{Inrush}}(t) = \sqrt{3} \cdot V_{\mathrm{n}} \cdot i_{\mathrm{Inrush}}(t) \tag{10}$$

where V_{n} is the line voltage at the bus to which the transformer is connected and i_{Inrush} is the time-dependent inrush current according to (8). The model neglects the influence of current phase angle, simplifying the calculation of reactive power for use in RMS-domain system studies. Using the corresponding reactive power values, the estimated inrush behavior can be implemented directly in RMS simulation tools such as DIgSILENT PowerFactory by applying the time-dependent Q_{Inrush} profile to a load element [6].

III. Identification of Load Model Parameter Sets

An example procedure for parameterization of each individual model component using literature data is provided below.

A. Dynamic Load Model Parameterization

Average annual load model parameter sets from [7] and a detailed seasonal parameter set from [16] serve as reference for three grid types. Here, the literature data for Germany, Luxembourg and Albania correspond to semi-urban, industrial and rural grid areas [7]. The grouping of the seasonal parameters is shown in Table I. Using the proportional scaling factor λ_c the initially unavailable detailed seasonal parameters ${P_c}^{(s,t)}$ per country c, season s and time of day t are estimated as:

$${P_c}^{(s,t)} = \lambda_c \cdot {P_{\mathrm{DE}}}^{(s,t)} \quad with \quad \lambda_c = \frac{\overline{P}_c}{\overline{P}_{\mathrm{DE}}} \tag{11}$$

with average $\overline{P}_{\mathrm{DE}}$ and detailed seasonal ${P_{\mathrm{DE}}}^{(s,t)}$ parameters for Germany and average parameters $\overline{P}_c$ for Luxembourg and Albania. Table II provides the resulting detailed seasonal load model parameter sets ($DE_{\mathrm{s,t}}$, $LU_{\mathrm{s,t}}$, $AL_{\mathrm{s,t}}$). Table III further shows the annual load model parameter sets (DE_{a}, LU_{a}, AL_{a}) and the relative errors RE with respect to the seasonal values:

$$RE_c = \frac{\overline{P}_c - {P_c}^{(s,t)}}{{P_c}^{(s,t)}} \tag{12}$$

Strong seasonal variations, e.g. in frequency-dependence, result in elevated relative errors, which are disproportionately high for small initial values. Here, rural parameters deviate more from the semi-urban trend than industrial parameters.

TABLE I

Categories for detailed seasonal load model parameter sets.

Seasons		Time of Day	
Summer	Jun - Aug	Day	1:00 p.m. - 3:00 p.m.
Winter	Dec - Feb	Evening	6:00 p.m. - 9:00 p.m.
Spring / Fall	Mar - May / Sep - Nov	Night	1:00 a.m. - 4:00 a.m.

TABLE II

Detailed load model parameter sets for semi-urban, industrial and rural grids by season and time of day.

	Semi-Urban $DE_{\mathrm{s,t}}$ [16]									**Industrial $LU_{\mathrm{s,t}}$**									**Rural $AL_{\mathrm{s,t}}$**								
	Summer			Winter			Spring / Fall			Summer			Winter			Spring / Fall			Summer			Winter			Spring / Fall		
Par.	Day	Eve	Night	Day	Eve	Night	Day	Eve	Night	Day	Eve	Night	Day	Eve	Night	Day	Eve	Night	Day	Eve	Night	Day	Eve	Night	Day	Eve	Night
Z_{p}	0.21	0.21	0.17	0.31	0.30	0.21	0.27	0.26	0.20	0.16	0.16	0.13	0.23	0.23	0.16	0.20	0.20	0.15	0.36	0.36	0.29	0.54	0.52	0.36	0.47	0.45	0.35
I_{p}	-0.11	-0.17	-0.21	-0.06	-0.14	-0.24	-0.10	-0.17	-0.25	-0.08	-0.13	-0.16	-0.05	-0.11	-0.18	-0.08	-0.13	-0.19	0.03	0.04	0.05	0.01	0.03	0.06	0.02	0.04	0.06
P_{p}	0.90	0.96	1.04	0.76	0.84	1.03	0.83	0.91	1.05	0.92	0.97	1.03	0.82	0.88	1.02	0.88	0.93	1.04	0.61	0.60	0.66	0.45	0.45	0.58	0.51	0.51	0.59
Z_{q}	1.64	1.58	1.64	1.64	1.56	1.64	1.65	1.58	1.65	1.65	1.59	1.65	1.65	1.57	1.65	1.66	1.59	1.66	1.51	1.46	1.51	1.51	1.44	1.51	1.52	1.46	1.52
I_{q}	-1.77	-1.65	-1.90	-1.67	-1.51	-1.87	-1.74	-1.60	-1.91	-1.84	-1.71	-1.97	-1.73	-1.57	-1.94	-1.81	-1.66	-1.98	-1.35	-1.26	-1.45	-1.27	-1.15	-1.42	-1.32	-1.22	-1.45
P_{q}	1.13	1.07	1.26	1.02	0.95	1.23	1.09	1.02	1.26	1.19	1.12	1.32	1.08	1.00	1.29	1.15	1.07	1.32	0.84	0.80	0.94	0.76	0.71	0.91	0.80	0.76	0.93
k_{pf}	1.03	1.14	1.38	0.82	0.97	1.42	0.94	1.08	1.42	1.12	1.24	1.50	0.89	1.06	1.55	1.02	1.18	1.55	0.78	0.86	1.04	0.62	0.73	1.07	0.71	0.81	1.07
k_{qf}	0.11	0.22	0.70	0.08	0.26	0.94	0.17	0.33	0.92	0.16	0.32	1.01	0.12	0.37	1.36	0.25	0.48	1.33	-0.00	-0.01	-0.02	-0.00	-0.01	-0.02	-0.00	-0.01	-0.02
t_1	0.04	0.03	0.03	0.04	0.03	0.03	0.04	0.03	0.03	0.04	0.03	0.03	0.04	0.03	0.03	0.04	0.03	0.03	0.03	0.02	0.02	0.03	0.02	0.02	0.03	0.02	0.02
t_{pv}	0.11	0.09	0.07	0.13	0.10	0.08	0.12	0.09	0.08	0.10	0.08	0.06	0.12	0.09	0.07	0.11	0.08	0.07	0.09	0.07	0.05	0.10	0.08	0.06	0.09	0.07	0.06
t_{qv}	0.04	0.04	0.04	0.05	0.04	0.04	0.05	0.04	0.04	0.03	0.03	0.03	0.04	0.03	0.03	0.04	0.03	0.03	0.03	0.03	0.03	0.04	0.03	0.03	0.04	0.03	0.03
t_{pf}	0.55	0.67	0.81	0.38	0.55	0.83	0.52	0.63	0.83	0.52	0.64	0.77	0.36	0.52	0.78	0.45	0.60	0.79	0.26	0.31	0.38	0.18	0.26	0.38	0.22	0.29	0.39
t_{qf}	0.11	0.22	0.70	0.08	0.26	0.94	0.17	0.33	0.92	0.08	0.17	0.53	0.06	0.20	0.71	0.13	0.25	0.69	0.04	0.08	0.24	0.03	0.09	0.33	0.06	0.11	0.32
Q_0	0.43	0.46	0.46	0.41	0.45	0.45	0.41	0.45	0.45	0.42	0.45	0.45	0.40	0.44	0.44	0.40	0.44	0.44	0.45	0.48	0.48	0.43	0.47	0.47	0.43	0.47	0.47

979-8-3315-8138-1

TABLE III

AVERAGE ANNUAL LOAD MODEL PARAMETER SETS AND RELATIVE ERRORS WITH RESPECT TO THE DETAILED PARAMETER SETS.

Load Model		Semi-Urban		Industrial		Rural	
Component	Par.	DE_{a} [7]	RE_{DE}	LU_{a} [7]	RE_{LU}	AL_{a} [7]	RE_{AL}
ZIP Model	Z_{p}	0.1806	0.06–0.42	0.1365	0.05–0.41	0.3122	0.08–0.42
ZIP Model	I_{p}	-0.0779	0.22–0.69	-0.0585	0.17–0.69	0.0183	0.09–0.83
ZIP Model	P_{p}	0.8973	≤0.18	0.9220	≤0.12	0.6695	0.01–0.49
ZIP Model	Z_{q}	1.5177	0.03–0.08	1.5275	0.03–0.08	1.4005	0.03-0.08
ZIP Model	I_{q}	-1.7474	≤0.16	-1.8151	≤0.16	-1.3292	0.01–0.16
ZIP Model	P_{q}	1.2297	≤0.29	1.2876	≤0.29	0.9287	≤0.31
Frequency	k_{pf}	1.1319	0.01–0.38	1.2338	0.01–0.39	0.8531	0.01–0.38
Frequency	k_{qf}	0.5869	0.16–6.34	0.8463	0.16–6.05	-0.0150	≥0.25
Dynamics	t_1	0.0490	0.23–0.63	0.0468	0.17–0.56	0.0401	0.34–1.01
Dynamics	t_{pv}	0.1022	0.02–0.46	0.0939	0.04–0.57	0.0796	0.01–0.59
Dynamics	t_{qv}	0.1087	1.17–1.72	0.0803	1.01–1.68	0.0928	1.32–2.09
Dynamics	t_{pf}	0.8827	0.06–1.32	0.8405	0.06–1.33	0.4117	0.77–0.89
Dynamics	t_{qf}	0.6789	0.03–7.49	0.5109	0.04–7.52	0.2354	0.22–0.93
Q Demand	Q_0	0.3919	0.04–0.15	0.3794	0.05–0.16	0.4082	0.05–0.15

All calculated numerical values are rounded to two decimal places.

B. Cold Load Pickup Model Parameterization

CLPU model parameterization has been widely investigated in the literature using both empirical data and simulation-based approaches. For instance, [4] analyzes 31 real reconnection events in Austria and Germany and provides fitted parameters for ED and DED models as published in [23]. An earlier study, [24], derives parameter ranges for the ED model from ten measured medium-voltage feeder events in Germany. While [8] does not provide explicit parameters, it offers a comprehensive discussion of typical CLPU magnitudes and underlying mechanisms such as diversity loss and inrush currents, which support modeling assumptions. Field-based insights are further contributed by [13], which examines residential CLPU behavior in Swedish networks through dedicated measurement campaigns. Simulation-based studies such as [15], [25] employ physical load modeling to reproduce the CLPU phenomenon.

Fig. 3 illustrates the modeled dynamic load behavior representing the CLPU effect during power restoration for both ED and DED models using parameters provided by [4].

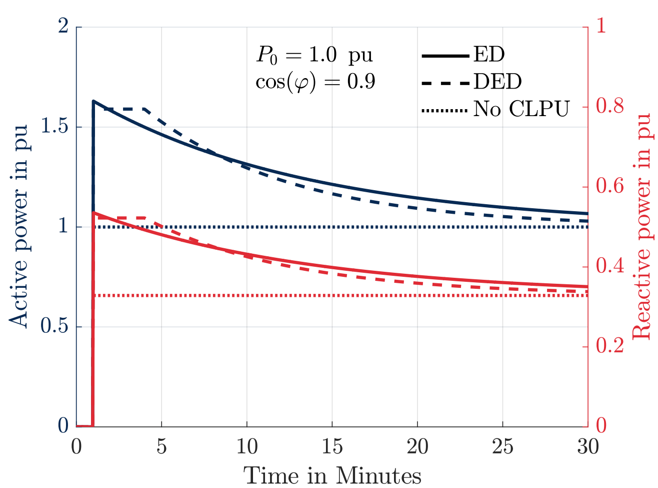

Fig. 3. CLPU effect per ED and DED model parameters from [4], Table 1: α_{ED} = 0.63 pu, τ_{ED} = 776 s, α_{DED} = 0.59 pu, τ_{DED} = 521 s and t_{d} = 180 s.

C. Transformer Inrush Current Model Parameterization

A dataset of 240 transformer inrush current measurements, corresponding to setup 00–05 of [26], serves as reference. The data was obtained from a single transformer configuration connected to the public grid, including two transformers (250 kVA and 400 kVA) tested under three loading conditions (no load, 48 kW and 102 kW). 40 measurements were recorded to capture the effect of switching phase-angle variations on the inrush current. In this study, all 240 measurements are used to derive the parameters of the model introduced in (8). For each measurement, three-phase current waveforms are evaluated over 200 cycles.

Each phase is first analyzed individually to determine the cycle-by-cycle peak-to-peak ($I_{\mathrm{p2p,1ph,c}}$), peak ($I_{\mathrm{peak,1ph,c}}$) and RMS ($I_{\mathrm{rms,1ph,c}}$) values. The three-phase data is combined into single representative signals for each quantity using the quadratic mean, yielding equivalent three-phase profiles $I_{\mathrm{p2p,3ph,c}}$, $I_{\mathrm{peak,3ph,c}}$, and $I_{\mathrm{rms,3ph,c}}$. This ensures subsequent analysis and parameter fitting are based on unified three-phase quantities rather than individual phase traces.

The time-dependent peak-to-peak envelope ($I_{\mathrm{p2p,3ph,c}}$) is used to fit the exponential function, as it naturally exhibits an exponential trend [19] and provides a stable basis for estimating the decay time constant t_{i}. The steady-state current I_{S} is obtained as the average RMS value per cycle over the final 10% of the record ($I_{\mathrm{rms,3ph,c}}$), representing the residual current level after inrush settling, alternatively it can be calculated based on the transformer loading. The relative amplitude ratio i_P represents initial inrush peak I_{Peak} of $I_{\mathrm{peak,3ph,c}}$ normalized by I_{S}. The method used to derive the parameters of the proposed model is illustrated in Fig. 4, where all quantities are normalized with respect to the transformer rated apparent power ($I_{\mathrm{norm}} = \frac{I \cdot \sqrt{3} \cdot V_{\mathrm{n}}}{S_{\mathrm{n}}}$). This normalization ensures consistent parameterization across transformer ratings and operating conditions and provides a conservative estimate of the maximum inrush magnitude and decay for RMS-based studies, rather than waveform accuracy.

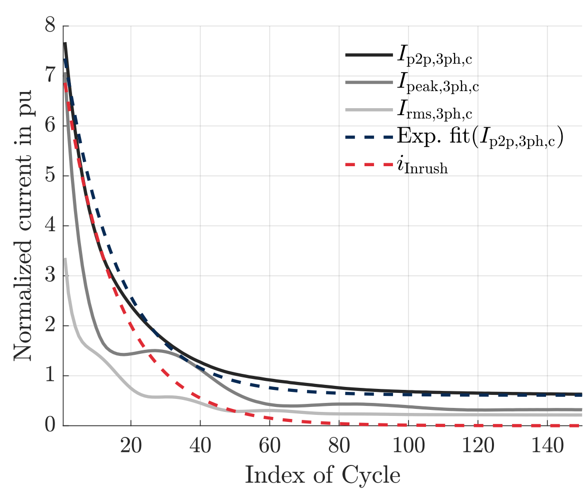

Fig. 4. Parameter derivation method for the proposed transformer inrush current model for i_{Inrush} (8), with: i_{p} = 33.4 pu, I_{S} = 0.2 pu and t_{i} = 15.5 s.

The left plot of Fig. 5 shows the extracted values for i_p and t_i from the inrush envelopes, characterizing inrush behavior for the considered transformer types and loading conditions. The highest peak ratios are observed under no-load conditions, reflecting the inherent nature of a ratio metric, whereas the lowest values occur at higher loading levels. This trend is consistent across both transformer types. In contrast, the right-hand plot shows the normalized initial peak current I_Peak versus t_i, exhibiting a different trend. This highlights the need for caution when interpreting inrush behavior based solely on i_p and t_i. Parameters from Fig. 4 are marked (★) for reference.

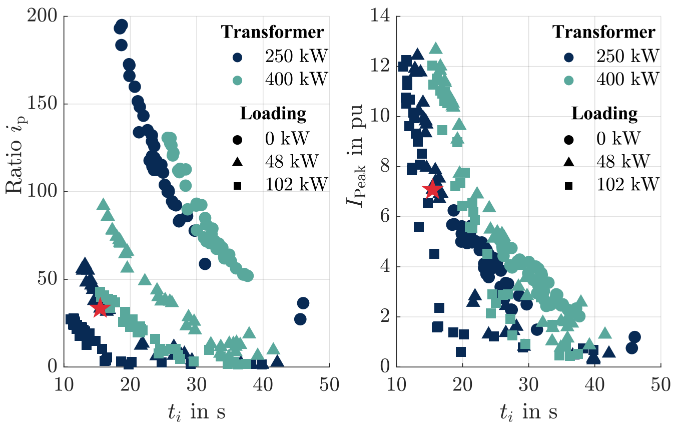

Fig. 5. Left: Ratio i_p versus time constant t_i. Right: Normalized I_Peak versus time constant t_i. Both for the evaluated inrush transformer data, for $t_\mathrm{i} \leq 50\ s$.

IV. Conclusion

This study has introduced an aggregated load modeling approach for dynamic power restoration studies, building on existing modeling approaches. By balancing accuracy and computational efficiency, the proposed approach preserves essential system dynamics while remaining suitable for large-scale RMS simulations. Owing to the limited number of parameters required for the CLPU and transformer inrush components, the model can be efficiently adapted to diverse system conditions. Unlike detailed composite load models, which require extensive data and computational resources, the proposed approach provides a simplified yet physically consistent representation of aggregated load behavior. However, it inevitably sacrifices detail at feeder and appliance levels, limiting its accuracy for highly localized analyses. The transformer inrush model is restricted to the decay characteristics and does not account for harmonic contents or residual flux distributions. The proposed approach relies on literature-based parameter values and representative sample measurement data, with further simulation-based analyses planned as future work.

References

[1] A. Arif *et al.*, "Load modeling—a review," *IEEE Transactions on Smart Grid*, vol. 9, no. 6, pp. 5986–5999, 2018.

[2] M. Mohammed, A. Abdulkarim, A. S. Abubakar, A. B. Kunya, and Y. Jibril, "Load modeling techniques in distribution networks: A review," *Journal of Applied Materials and Technology*, vol. 1, no. 2, pp. 63–70, 2020.

[3] R. Benato *et al.*, "A novel dynamic load modeling for power systems restoration: An experimental validation on active distribution networks," *IEEE Access*, vol. 10, pp. 89861–89875, 2022.

[4] C. Hachmann, H. Becker, and M. Braun, "Cold load pickup model adequacy for power system restoration studies," *Energies*, vol. 15, no. 20, p. 7675, 2022.

[5] W. Price *et al.*, "Load representation for dynamic performance analysis," *IEEE Transactions on Power Systems*, vol. 8, no. 2, pp. 472–482, 1993.

[6] DIgSILENT GmbH, "PowerFactory2024: Technical Reference - General Load (ElmLod, TypLod)," 2024.

[7] D. Stenzel and R. Witzmann, "Modelling the aggregate load behaviour of european regions and its influence on dynamic and static voltage stability," in *CIRED 2021 - The 26th International Conference and Exhibition on Electricity Distribution*, pp. 2391–2395, IET, 2021.

[8] "PES-TR38: Cold load pickup issues," tech. rep., IEEE PES, Power System Relay Committee, Line Protection Subcommittee, 2004.

[9] "Understanding and mitigating cold-load pickup issues following a long duration power outage," tech. rep., EPRI, 2023.

[10] "Cold load pickup," tech. rep., UK Power Networks, 2022.

[11] F. Bu, K. Dehghanpour, Z. Wang, and Y. Yuan, "A data-driven framework for assessing cold load pick-up demand in service restoration," *IEEE Transactions on Power Systems*, vol. 34, no. 6, pp. 4739–4750, 2019.

[12] M. Gonzalez, K. A. Wheeler, and S. O. Faried, "An overview of cold load pickup modeling for distribution system planning," in *2021 IEEE Electrical Power and Energy Conference (EPEC)*, (Toronto, ON, Canada), pp. 328–333, 2021.

[13] E. Agneholm and J. Daalder, "Cold load pick-up of residential load," *IEE Proceedings - Generation, Transmission and Distribution*, vol. 147, no. 1, pp. 44–50, 2000.

[14] Y. Li, W. Sun, W. Yin, S. Lei, and Y. Hou, "Restoration strategy for active distribution systems considering endogenous uncertainty in cold load pickup," *IEEE Transactions on Smart Grid*, vol. 13, no. 4, pp. 2690–2702, 2022.

[15] K. P. Schneider, E. Sortomme, S. S. Venkata, M. T. Miller, and L. Ponder, "Evaluating the magnitude and duration of cold load pick-up on residential distribution feeders using multi-state load models," *IEEE Transactions on Power Systems*, vol. 31, no. 5, pp. 3765–3774, 2016.

[16] D. Stenzel *et al.*, "Modelling of stationary and dynamic demand behavior considering sectoral and regional characteristics," in *CIRED 2019 - The 25th International Conference and Exhibition on Electricity Distribution*, 2019.

[17] A. Winkens *et al.*, "Does transformer inrush challenge future grids? – laboratory insights," in *CIRED 2023 - The 27th International Conference and Exhibition on Electricity Distribution*, pp. 2479–2483, IET, 2023.

[18] C. L. Cheng, C. E. Lin, C. L. Huang, and J. C. Yeh, "A simple model for transformer inrush current calculation and harmonic analysis," *Electric Power Systems Research*, vol. 24, no. 2, pp. 153–163, 1992.

[19] J. E. Holcomb, "Distribution transformer magnetizing inrush current," *Transactions of the American Institute of Electrical Engineers, Part III: Power Apparatus and Systems*, vol. 80, no. 3, pp. 697–702, 1961.

[20] A. Moradi and S. M. Madani, "Technique for inrush current modelling of power transformers based on core saturation analysis," *IET Generation, Transmission & Distribution*, vol. 12, no. 10, pp. 2317–2324, 2018.

[21] Z. Taghikhani, M. A. Taghikhani, and G. B. Gharehpetian, "Inrush current modeling of three-limb core-type power transformers based on efficient analytical–numerical hybrid method," *International Journal of Electrical Power & Energy Systems*, vol. 117, p. 105694, 2020.

[22] C. Carrander, *Magnetizing Currents in Power Transformers – Measurements, Simulations, and Diagnostic Methods*. PhD thesis, KTH Royal Institute of Technology, Stockholm, Sweden, 2017.

[23] Universität Kassel, Fachgebiet Nachhaltige Elektrische Energiesysteme, "Cold load pickup (CLPU) time series and statistics," 2022. https://www.uni-kassel.de/eecs/e2n/unsere-entwicklungen/daten-und-modelle.html. [Online] Accessed Oct. 2, 2025.

[24] C. Hachmann, G. Lammert, L. Hamann, and M. Braun, "Cold load pickup model parameters based on measurements in distribution systems," *IET Generation, Transmission & Distribution*, vol. 13, no. 23, pp. 5387–5395, 2019.

[25] D. Raoofsheibani *et al.*, "Residual load models for power system restoration: High shares of residential thermal loads and volatile pv generators," in *2017 IEEE International Conference on Smart Grid Communications*, (Piscataway, NJ), pp. 223–228, IEEE, 2017.

[26] A. Winkens *et al.*, "Transformer inrush measurements in a distribution grid laboratory." Zenodo, 2023. https://zenodo.org/records/7712948. [Online] Accessed Nov. 4, 2025.

979-8-3315-8138-1